Published in final edited form as:
Am J Med Genet A. 2010 December ; 152A(12): 3074–3083. doi:10.1002/ajmg.a.33733.

Recurrent interstitial 1p36 deletions: evidence for germline mosaicism and complex rearrangement breakpoints

Marzena Gajecka[1,*], **Sulagna C. Saitta**[2,3,*], **Andrew J. Gentles**[4], **Lindsey Campbell**[2], **Karen Ciprero**[2], **Elizabeth Geiger**[2], **Anne Catherwood**[2], **Jill A. Rosenfeld**[5], **Tamim Shaikh**[2,3,**], and **Lisa G. Shaffer**[5]

[1] Institute of Human Genetics, Polish Academy of Sciences, Poznan, Poland [2] Division of Human Genetics, The Children's Hospital of Philadelphia, Philadelphia, PA, USA [3] Department of Pediatrics, University of Pennsylvania School of Medicine, Philadelphia, PA, USA [4] School of Medicine, Stanford University, Stanford, CA, USA [5] Signature Genomic Laboratories, Spokane, WA, USA

Abstract

Deletions of chromosome 1p36 are one of the most frequently encountered subtelomeric alterations. Clinical features of monosomy 1p36 include neurocognitive impairment, hearing loss, seizures, cardiac defects, and characteristic facial features. The majority of cases have occurred sporadically, implying that genomic instability plays a role in the prevalence of the syndrome. Here we report two siblings with mild phenotypic features of the deletion syndrome, including developmental delay, hearing loss and left ventricular noncompaction (LVNC). Microarray analysis using bacterial artificial chromosome and oligonucleotide microarrays indicated the deletions were identical, suggesting germline mosaicism. Parental phenotypes were normal, and analysis by fluorescence *in situ* hybridization (FISH) did not show mosaicism. These small interstitial deletions were not detectable by conventional subtelomeric FISH analysis. To investigate the mechanism of deletion further, the breakpoints were cloned and sequenced, demonstrating the presence of a complex rearrangement. Sequence analysis of genes in the deletion interval did not reveal any mutations on the intact homologue that may have contributed to the LVNC seen in both children. This is the first report of apparent germline mosaicism for this disorder. Thus, our findings have important implications for diagnostic approaches and for recurrence risk counseling in families with a child with monosomy 1p36. In addition, our results further refine the minimal critical region for LVNC and hearing loss.

Keywords

1p36; deletion; germline mosaicism; LVNC; hearing loss

INTRODUCTION

Monosomy of chromosome band 1p36 has an estimated incidence of 1 in 5000 live births and may be the most frequently occurring subtelomeric deletion syndrome [Heilstedt et al., 2003a]. The clinical presentation is variable and includes characteristic facial features such

For correspondence and reprints: Lisa G. Shaffer, Ph.D., Signature Genomic Laboratories, 2820 N. Astor St., Spokane, WA 99207, Ph : 509.474.6840, Fax : 509.474.6839, shaffer@signaturegenomics.com.
*These authors contributed equally.
**Current affiliation: Department of Pediatrics, University of Colorado Denver, Aurora, CO

as deepset eyes, straight eyebrows, depressed nasal bridge and midface hypoplasia, as well as a range of clinical and cognitive issues including hypotonia, hearing loss, hypothyroidism, seizure disorder, congenital cardiac defects, global developmental delay and/or mental retardation [Gajecka et al., 2007; Battaglia et al., 2008]. Many individuals with monosomy 1p36 are non-verbal, whereas others have preserved but delayed expressive language [Battaglia, 2005].

The majority of deletions arise *de novo*, with about 3% attributable to malsegregation of a balanced parental translocation [Gajecka et al., 2007]. The size of the deletion is variable from submicroscopic (< 5 Mb) to as large as 32 Mb. There appears to be a correlation between the size of the deletion and severity of some clinical features [Heilstedt et al., 2003b], although there is no correlation between the deletion size and the number of observed clinical features [Gajecka et al., 2007]. Even patients with deletions <3 Mb can present with most of the features associated with monosomy 1p36 [Gajecka et al., 2007]. Of the *de novo* terminal deletions for which parental origin is known, 52.7% are maternal in origin, and 47.3% are paternal. Deletions larger than 5 Mb tend to be paternal in origin. In contrast, 83.3% of interstitial deletions previously investigated are maternal in origin [Gajecka et al., 2007]. The mode of inheritance is primarily sporadic, and, other than deletions arising from malsegregation of a balanced parental translocation, familial deletions have not been described.

We report on a pair of siblings with interstitial 1p36 deletion. Both siblings display mild manifestations of monosomy 1p36. The parent of origin of the deletion for both children was the same, suggestive of maternal germline mosaicism as the mechanism of recurrence. Further, this is the first report of familial recurrence involving an interstitial deletion resulting in monosomy 1p36, which reinforces that the risk of germline mosaicism should be emphasized when counseling families with a new diagnosis in a child with monosomy 1p36.

CLINICAL REPORTS

Patient 1 was previously reported [Ming et al., 2006]. She presented for genetics evaluation due to cardiomyopathy and bifid uvula. She was born at 41 weeks gestation via spontaneous vaginal delivery to a G1P0-1 mother following an uncomplicated pregnancy. Birth weight was 3.29 kg (50^{th} centile) and birth length was 53.4 cm ($>90^{th}$ centile). The neonatal history was significant for hypoglycemia noted on day 2 of life, failed newborn hearing screen, and low heart rate followed by a normal electrocardiogram (EKG). At age 3 months, the patient developed pulmonary edema and was subsequently diagnosed with cardiomyopathy. Cardiac evaluation and multiple echocardiograms demonstrated left ventricle non-compaction (LVNC) of the free wall and apex as well as aortic regurgitation, trivial tricuspid regurgitation, borderline normal left ventricle shortening and mild left ventricular dysfunction with dilated cardiomyopathy. Treatment with carvedilol, a beta-blocker, was initiated, and the child has remained clinically stable since, with no further medications or interventions required. Additional studies included a normal head CT, renal ultrasound and normal lumbar spine MRI to evaluate a sacral hair tuft. Renal ultrasound indicated normal kidney structure and positioning.

Developmental milestones were delayed. Patient 1 walked at 19 months of age and had initial expressive speech delay with poor articulation. Developmental evaluation at 19 months of age showed cognitive, social, emotional and fine motor skills at the 14–15-month level, receptive communication at the 18-month level and expressive communication at the 13–15-month level with gross motor skills delayed at an equivalent of 10 months. When examined at age 5 years, the patient had no history of seizures. Follow-up audiometry testing showed moderate bilateral sensorineural hearing loss in the high-frequency ranges.

More recently, mild conductive hearing loss was diagnosed, and she currently wears hearing aids. At age 5 years, significant progress was noted with cognitive, social, emotional, and fine motor skills in the 4.5–5-year range and expressive language in the 4–4.5-year range.

Physical exam showed a normal head circumference and age-appropriate growth parameters. The exam was significant for generalized ligamentous laxity including decreased hip rotation and joint movement including pronation of the ankles. There is no history of fractures or dislocations. There was evidence of truncal hypotonia and low foot arches. The proposita developed dark body hair at approximately 4 years of age. Dysmorphic features were minimal and included upslanting palpebral fissures, characteristic eyebrows and a slightly depressed nasal bridge with minimal midfacial flattening (Fig 1).

Patient 2 is the younger sister of Patient 1. Patient 2 presented for genetics evaluation at age 1 month because of parental concerns that she resembled her sister. Her newborn hearing screen was noted to be abnormal, and a sacral hair tuft was noted at birth. On exam, Patient 2 had mid-facial flattening, a depressed nasal bridge and mildly upslanting palpebral fissures but was otherwise morphologically normal. She had normal growth parameters on exam. After the diagnosis of a 1p36 deletion, an echocardiogram revealed mild non-compaction cardiomyopathy, which, unlike her sister's, was clinically silent and did not require medication or intervention. The history of Patient 2 is also significant for hypotonia, bilateral sensorineural hearing loss, and premature thelarche evident by age 18 months.

On physical exam at 19 ½ months, growth parameters showed height at the 5th centile, weight less than the 5th centile, and head circumference at the 5^{th} – 10^{th} centile. Developmental milestones were delayed; the patient rolled at 5 months of age, crawled at 13 ½ months of age, began pulling to stand at 15 months of age, and started cruising at 16 months of age. She was not yet walking at 19 ½ months and used both verbal communication and sign language, with approximately two verbal single-syllable words and 25 or more signs. She had good receptive language and could follow commands.

MATERIALS AND METHODS

Cytogenetic analyses

Microarray-based comparative genomic hybridization (aCGH) was performed at Signature Genomic Laboratories according to published methods [Bejjani et al., 2005; Ballif et al., 2008a]. Fluorescence *in situ* hybridization (FISH) was performed according to published methods [Shaffer et al., 1994] using probe RP11-740P5 from 1p36 to confirm the interstitial deletion in Patient 2. FISH was performed on both parents to exclude a deletion, and multiple FISH probes were used to rule out evidence of a cryptic translocation.

Microarray Analysis and Breakpoint Refinement

The deletion in Patient 1 was first detected using an Affymetrix 100K array and previously reported [Ming et al., 2006]. Both patients were also analyzed using Illumina HumanHap 550K microarrays (Illumina Inc. San Diego, CA) as previously described [Haldeman-Englert et al., 2009]. To refine the breakpoints in both deletions, both patients were re-analyzed using an off-the-shelf 244K-feature whole-genome oligonucleotide microarray (Agilent Technologies, Santa Clara, CA), as previously described [Ballif et al., 2008b].

Cloning and Sequencing of the Breakpoints

To perform further sequence-level analyses, somatic cell hybrids from Patient 1 were generated as previously described [Page and Shaffer, 1997], and hybrids containing either the deleted chromosome 1 or the normal homologue were identified after screening with

microsatellite markers and FISH as previously described [Page and Shaffer, 1997]. To identify the 1p36 interstitial deletion breakpoints, sequence tagged site (STS) markers were designed and PCR analyses performed using DNA from the deleted chromosome 1 hybrid using published methods [Gajecka et al., 2006a]. PCR primers were designed based on sequences in GenBank (www.ncbi.nlm.nih.gov) and corresponded to the genomic region containing the 1p36 breakpoints of Patient 1. Repetitive elements were masked from the sequence using Repeat Masker (http://www.repeatmasker.org/), and 200–400 bp STS markers were then designed from the unmasked unique sequence using Primer 3 (http://frodo.wi.mit.edu/cgi-bin/primer3/primer3_www.cgi). Both 1p36 breakpoints were narrowed using markers spaced ~20 kb apart along the length of the chromosome, narrowed to ~5 kb apart, ~1 kb apart and finally 400 bp apart. Breakpoints were identified in the sequence corresponding to that contained in BACs RP11-547D24 (AL391845, distal breakpoint; B1) and RP11-46F15 (AL513320, proximal breakpoint, B2). We then designed a forward PCR primer from the putative 1p36 distal breakpoint and reverse primer from unique sequence located at the putative proximal breakpoint to amplify across the junction. The putative junction fragment was sequenced using an ABI PRISM 3100-Avant genetic analyzer and Big Dye reagents (Applied Biosystems, Carlsbad, CA) as previously described [Ballif et al., 2004]. Sequencher 4.6 (Gene Codes, Ann Arbor, MI) was used to analyze sequence on either side of the breakpoint junctions. The original chromosomal sequences from which the deletion breakpoints originate were identified using BLAT [Kent, 2002] from the UCSC Genome Browser website (http://genome.ucsc.edu), and the breakpoint sequences and 200 bp of adjacent flanking sequence were compared and analyzed.

Genotype analysis within the deletion region was performed on Patient 1's genomic DNA, and analysis of DNA outside the deleted region was performed on hybrids by comparison to parental genotypes with microsatellite marker D1S243.

No hybrids were established for Patient 2. Instead, the primers used in experiments for patient 1 were applied to amplify the junction across the deletion in patient 2. We used a unique-sequence forward primer located 200–300 bp from the B1 breakpoint in patient 1 and a reverse primer from the B2 breakpoint in Patient 1. The sequence junction in Patient 2 was amplified using DNA extracted from peripheral blood.

Sequence motifs at the junctions were identified as described elsewhere [Gajecka et al., 2008]. We searched for putative regions of Z-DNA structure using Z-Hunt [Clamp et al., 2004; http://gac-web.cgrb.oregonstate.edu/zDNA/] and for sequence motifs potentially predisposing to rearrangement formation using the "fuzznuc" program from EMBOSS [Rice et al., 2000]. Potentially relevant motifs such as vertebrate topoisomerase consensus cleavage sites [RNYNNCNNGYNGKTNYNY], translin sites [GCCCWSSW and ATGCAG], DNA polymerase a/b frameshift hotspots [ACCCWR, TGGNGT, GGGGGA, TCCCCC, and CTGGCG], and deletion hotspot consensus sequences [TGRRKM] were considered [Gajecka et al., 2008]. Inverted repeats in sequences were analyzed using the "palindrome" program of EMBOSS. Direct repeats were identified with Tandem Repeats Finder [Benson, 1999] using default parameters. Oligopurine (R) and oligopyrimidine (Y) tracts were analyzed by translating the nucleotide sequences into the R/Y alphabet, and locating the longest tracts occurring in the breakpoint regions. To examine whether the sequences near the breakpoints can form cruciform structures, we used UNAFold [Markham and Zuker, 2008] to display potential configurations.

Sequencing of Genes in the Deleted Region

Left ventricular non-compaction (LVNC) was present in both children, although it was subclinical in Patient 2. Both parents received echocardiograms and did not demonstrate evidence of non-compaction. Because this specific cardiac defect has been previously

associated with some cases of deletion 1p36 [Thienpont et al., 2007; Battaglia et al., 2008], we studied whether the deletion permitted expression of a recessive allele inherited from a parent. In all family members, we sequenced all exons and intron-exon boundaries of *PANK4*, *HES5*, and *SKI*, all located within the deletion interval. Primers used are shown in Table I.

RESULTS

Microarray analysis performed on both patients identified an interstitial deletion in the distal short arm of chromosome 1, approximately 1.5 Mb in size. This deletion begins 1.9 Mb from the 1p terminus (RP11-547D24, AL391845) and extends to approximately 3.4 Mb from the 1p terminus (RP11-168F9, AL512413). High-resolution microarray analysis using a 244K-feature oligonucleotide microarray showed the deletions were ~1.51 Mb in size (chr1:1,906,449–3,419,622, hg18 coordinates). FISH confirmed the deletion in both patients (Fig 2). FISH analysis using BAC clone RP11-740P5 on parental blood specimens showed a normal hybridization pattern in both parents.

Genotype analysis revealed a maternal origin for each deletion, which was confirmed by comparative sequence analysis in patients and their parents on the genomic and hybrid DNA. Figure 3 illustrates the complex rearrangement present at the junction. An approximately 1.52 Mb deletion was identified, consistent with two short sequence insertions at the breakpoint junction. Patient 2 had the same rearrangement at 1p36 with the same breakpoints and insertions as Patient 1 (Fig 3). Amplification of the breakpoints was attempted on DNA extracted from peripheral blood on the mother and failed to amplify, indicating no evidence of the interstitial deletion in the mother's blood.

Sequence analysis of the deletion breakpoints is shown in Figure 4. Vertebrate topoisomerase consensus cleavage site, translin sites, deletion hotspot consensus sequences and DNA polymerase a/b frameshift hotspots were identified (Fig 4). No putative regions of Z-DNA structure were identified in the breakpoint junctions.

To investigate potentially relevant secondary structures as a cause of double-strand breaks, we performed UNAfold analysis for fragments of normal chromosome sequences involved in the rearrangement. We did not find these structures to be particularly helpful for understanding the mechanisms. Furthermore, no putative regions of Z-DNA structure were identified in the breakpoint junctions. These results are similar to our previous data on monosomy 1p36 breakpoints and junctions [Gajecka et al., 2008].

B2 is localized in human gene *MEGF6* [multiple epidermal growth factor-like domains 6 precursor (EGF-like domain-containing protein 3) (Multiple EGF-like domain protein 3); OMIM 604266]. B1 is localized in human gene *KIAA1751* (hypothetical protein LOC85452).

DISCUSSION

This is the first case of recurrent monosomy 1p36 observed in siblings secondary to potential germline mosaicism. Both parents are phenotypically normal and showed normal FISH patterns on metaphase analysis. Given the identical deletions in the siblings with the same parental origin, the mechanism is most consistent with germline mosaicism. Because the deletion is small (1.52 Mb) and interstitial, it is not detectable by subtelomere FISH analysis, which is typically informative in terminal deletions. The patients display mild phenotypes with mild cognitive differences but no seizures or hypothyroidism. The craniofacial exam does reflect some of the features associated with monosomy 1p36 such as midfacial hypoplasia, downslanting lateral aspect of the eyebrows, and upslanting palepebral

fissures. The findings underscore the utility of an aCGH-based approach for diagnosing chromosome abnormalities.

Our results also further refine the minimal critical region for a number of the phenotypic features of monosomy 1p36, particularly for hearing loss and LVNC. LVNC has been described in several patients with 1p36 terminal deletions >5 Mb [Thienpont et al., 2007; Cremer et al., 2008; Dod et al., 2010]. Therefore, our patients' deletion represents the smallest deletion associated with LVNC and can help narrow the search for a causative gene(s). LVNC is a failure of myocardial morphogenesis, resulting in clefts or trabeculations in the left ventricle of the heart and poor systolic function. Other loci are also associated with LVNC including *LVNC1* (*DTNA*) on chromosome 18, which encodes a gene that contributes to an autosomal dominant form, and *LVNX* (*TAZ*) on the X chromosome which encodes the tafazzin gene in an X-linked form [Finsterer, 2009]. Patient 1 had been enrolled in a separate research protocol testing for these genes and no pathogenic mutations of *LVNC1* or *LVNCX* were reported (Ming JE, personal communication). We did not find evidence for additional mutations in genes in the deleted 1p36 region of these patients to attribute this feature to a recessive form of disease. We specifically tested *PANK4*, a regulatory enzyme expressed mainly in muscle involved in CoA biosynthesis; *HES5*, a transcription factor expressed mainly in the central nervous system; and *SKI*, a member of the TGFB1 family that has been previously associated with dilated cardiomyopathy. The lack of pathogenic point mutations on the non-deleted allele does not rule out the possibility that haploinsufficiency of these genes by deletion can result in non-compaction of variable severity. Another candidate gene for LVNC is *PRKCZ*, which encodes an atypical protein kinase C (PKCζ) that has been shown to play a role in phosphorylation of cardiac sarcomeric proteins, including cardiac troponin I (cTnI) and troponin T (cTnT) [Wu and Solaro, 2007]. Mutations in *TNNT2*,which encodes cTnT, have been recently reported in association with familial LVNC [Klaassen et al., 2008; Luedde et al., 2010]. *PRDM16*, also in the deleted region, has been shown to play a role in heart development, as mutant mice have gross cardiac ventricular hypoplasia and occasional clefting between the ventricles [Bjork et al., 2010].

The relatively small size of our patients' deletion also allows for a narrower search of candidate genes for the hearing loss associated with monosomy 1p36. The terminal ~2.9 Mb of the chromosome has been proposed as a critical region for hearing loss [Heilstedt et al., 2003b], although an interstitial 7 Mb deletion starting within the *PRDM16* gene ~3.1 Mb from the telomere has also been reported in an individual with hearing loss [Redon et al., 2005]. Our patients' deletion overlaps both of these regions. *HES5* is in the previously described terminal region, and it has been shown to play a role in proper cochlear hair cell development [Zine et al., 2001; Hartman et al., 2009]. *ACTRT2*, which is at the end of the previously described terminal critical region, and *ARHGEF16*, which is within the overlapping region with the interstitial deletion, both may play roles in cytoskeletal organization [Harata et al., 2001; Jiang et al., 2006; Popoff and Geny, 2009], and several forms of hereditary deafness, including DFNA1, are associated with cytoskeleton function [Dror and Avraham, 2009]. Given the non-overlapping nature of some of the 1p36 deletions associated with hearing loss, multiple genes may be responsible for or contribute to the hearing loss in the syndrome.

The junction fragment analysis revealed that the breakpoints interrupt a gene and predicted protein in this rearrangement. Several genes are deleted in these patients (Table II). Thus, the significance of the gene disruptions/deletions with respect to LVNC or hearing loss is unknown.

The deletion breakpoints were analyzed at the sequence level and found to be complex, showing an interstitial deletion with retention of small intervening noncontiguous sequences. These results are similar to those found in other cloned breakpoints in monosomy 1p36 examined with high-resolution techniques [Gajecka et al., 2006b; Gajecka et al., 2008].

Sequence motifs have been associated with genomic rearrangements and have been identified as factors influencing DNA breakage by non-B-DNA conformations [Chuzhanova et al., 2003; Bacolla et al., 2004; Bacolla and Wells, 2004; Raghavan and Lieber, 2006]. The sequence motifs identified here are similar to those recognized in other classes of 1p36 deletions. Based on only one rearrangement, the motif distribution cannot be determined; however, the motif density is similar to that observed in translocations in monosomy 1p36 [Gajecka et al., 2008].

Insertions of several base pairs and microhomology at the breakpoints are frequently observed at 1p36 junctions, as seen in the cases presented here. Microhomology and insertions are primary features of nonhomologous end-joining (NHEJ) mechanisms, which we have proposed to be the primary mechanism in the rearrangement formation in monosomy 1p36 [Gajecka et al., 2006b; Gajecka et al., 2008]. Additionally one of the insertions is in inverted orientation compared to the original 1p36 sequence. Thus, in this case, the FoSTes mechanism could be also applicable [Lee et al., 2007].

The identification of identical, complex interstitial deletions of maternal origin from a chromosomally normal mother is indicative of germline mosaicism. This case illustrates the importance of considering the possibility of germline mosaicism when counseling parents of children with apparently *de novo* chromosome anomalies. The identification of small deletions associated with mild dysmorphic features, hearing loss and LVNC narrows the critical region in which to search for causative genes. Identifying the causative genes may allow for the development of novel treatment targets for various features of the syndrome.

Acknowledgments

We thank Aaron Theisen, Signature Genomic Laboratories, for his careful editing of the manuscript and helpful suggestions. This work was partially supported by NIH grant GM081519 (THS).

References

Bacolla A, Jaworski A, Larson JE, Jakupciak JP, Chuzhanova N, Abeysinghe SS, O'Connell CD, Cooper DN, Wells RD. Breakpoints of gross deletions coincide with non-B DNA conformations. Proc Natl Acad Sci U S A. 2004; 101:14162–14167. [PubMed: 15377784]

Bacolla A, Wells RD. Non-B DNA conformations, genomic rearrangements, and human disease. J Biol Chem. 2004; 279:47411–47414. [PubMed: 15326170]

Ballif BC, Theisen A, Coppinger J, Gowans GC, Hersh JH, Madan-Khetarpal S, Schmidt KR, Tervo R, Escobar LF, Friedrich CA, McDonald M, Campbell L, Ming JE, Zackai EH, Bejjani BA, Shaffer LG. Expanding the clinical phenotype of the 3q29 microdeletion syndrome and characterization of the reciprocal microduplication. Mol Cytogenet. 2008a; 1:8. [PubMed: 18471269]

Ballif BC, Theisen A, McDonald-McGinn DM, Zackai EH, Hersh JH, Bejjani BA, Shaffer LG. Identification of a previously unrecognized microdeletion syndrome of 16q11.2q12.2. Clin Genet. 2008b; 74:469–475. [PubMed: 18811697]

Ballif BC, Wakui K, Gajecka M, Shaffer LG. Translocation breakpoint mapping and sequence analysis in three monosomy 1p36 subjects with der(1)t(1;1)(p36;q44) suggest mechanisms for telomere capture in stabilizing de novo terminal rearrangements. Hum Genet. 2004; 114:198–206. [PubMed: 14579147]

Battaglia A. Del 1p36 syndrome: a newly emerging clinical entity. Brain Dev. 2005; 27:358–361. [PubMed: 16023552]

Battaglia A, Hoyme HE, Dallapiccola B, Zackai E, Hudgins L, McDonald-McGinn D, Bahi-Buisson N, Romano C, Williams CA, Brailey LL, Zuberi SM, Carey JC. Further delineation of deletion 1p36 syndrome in 60 patients: a recognizable phenotype and common cause of developmental delay and mental retardation. Pediatrics. 2008; 121:404–410. [PubMed: 18245432]

Bejjani BA, Saleki R, Ballif BC, Rorem EA, Sundin K, Theisen A, Kashork CD, Shaffer LG. Use of targeted array-based CGH for the clinical diagnosis of chromosomal imbalance: Is less more? Am J Med Genet A. 2005; 134:259–267. [PubMed: 15723295]

Benson G. Tandem repeats finder: a program to analyze DNA sequences. Nucleic Acids Res. 1999; 27:573–580. [PubMed: 9862982]

Bjork BC, Turbe-Doan A, Prysak M, Herron BJ, Beier DR. Prdm16 is required for normal palatogenesis in mice. Hum Mol Genet. 2010; 19:774–789. [PubMed: 20007998]

Chuzhanova N, Abeysinghe SS, Krawczak M, Cooper DN. Translocation and gross deletion breakpoints in human inherited disease and cancer II: Potential involvement of repetitive sequence elements in secondary structure formation between DNA ends. Hum Mutat. 2003; 22:245–251. [PubMed: 12938089]

Clamp M, Cuff J, Searle SM, Barton GJ. The Jalview Java alignment editor. Bioinformatics. 2004; 20:426–427. [PubMed: 14960472]

Cremer K, Ludecke HJ, Ruhr F, Wieczorek D. Left-ventricular non-compaction (LVNC): a clinical feature more often observed in terminal deletion 1p36 than previously expected. Eur J Med Genet. 2008; 51:685–688. [PubMed: 18721913]

Dibbens LM, Feng HJ, Richards MC, Harkin LA, Hodgson BL, Scott D, Jenkins M, Petrou S, Sutherland GR, Scheffer IE, Berkovic SF, Macdonald RL, Mulley JC. GABRD encoding a protein for extra- or peri-synaptic GABAA receptors is a susceptibility locus for generalized epilepsies. Hum Mol Genet. 2004; 13:1315–1319. [PubMed: 15115768]

Dod HS, Bhardwaj R, Hummel M, Morise AP, Batish S, Warden BE, Beto RJ, Jain AC. Left ventricular noncompaction: a rare disorder in adults and its association with 1p36 chromosomal anomaly. Am J Med Genet A. 2010; 152A:191–195. [PubMed: 20034097]

Dror AA, Avraham KB. Hearing loss: mechanisms revealed by genetics and cell biology. Annu Rev Genet. 2009; 43:411–437. [PubMed: 19694516]

Finsterer J. Cardiogenetics, neurogenetics, and pathogenetics of left ventricular hypertrabeculation/noncompaction. Pediatr Cardiol. 2009; 30:659–681. [PubMed: 19184181]

Gajecka M, Gentles AJ, Tsai A, Chitayat D, Mackay KL, Glotzbach CD, Lieber MR, Shaffer LG. Unexpected complexity at breakpoint junctions in phenotypically normal individuals and mechanisms involved in generating balanced translocations t(1;22)(p36;q13). Genome Res. 2008; 18:1733–1742. [PubMed: 18765821]

Gajecka M, Glotzbach CD, Jarmuz M, Ballif BC, Shaffer LG. Identification of cryptic imbalance in phenotypically normal and abnormal translocation carriers. Eur J Hum Genet. 2006a; 14:1255–1262. [PubMed: 16941016]

Gajecka M, Glotzbach CD, Shaffer LG. Characterization of a complex rearrangement with interstitial deletions and inversion on human chromosome 1. Chromosome Res. 2006b; 14:277–282. [PubMed: 16628498]

Gajecka M, Mackay KL, Shaffer LG. Monosomy 1p36 deletion syndrome. Am J Med Genet C Semin Med Genet. 2007; 145C:346–356. [PubMed: 17918734]

Haldeman-Englert CR, Gai X, Perin JC, Ciano M, Halbach SS, Geiger EA, McDonald-McGinn DM, Hakonarson H, Zackai EH, Shaikh TH. A 3.1-Mb microdeletion of 3p21.31 associated with cortical blindness, cleft lip, CNS abnormalities, and developmental delay. Eur J Med Genet. 2009; 52:265–268. [PubMed: 19100872]

Harata M, Nishimori K, Hatta S. Identification of two cDNAs for human actin-related proteins (Arps) that have remarkable similarity to conventional actin. Biochim Biophys Acta. 2001; 1522:130–133. [PubMed: 11750065]

Hartman BH, Basak O, Nelson BR, Taylor V, Bermingham-McDonogh O, Reh TA. Hes5 expression in the postnatal and adult mouse inner ear and the drug-damaged cochlea. J Assoc Res Otolaryngol. 2009; 10:321–340. [PubMed: 19373512]

Heilstedt HA, Ballif BC, Howard LA, Kashork CD, Shaffer LG. Population data suggest that deletions of 1p36 are a relatively common chromosome abnormality. Clin Genet. 2003a; 64:310–316. [PubMed: 12974736]

Heilstedt HA, Ballif BC, Howard LA, Lewis RA, Stal S, Kashork CD, Bacino CA, Shapira SK, Shaffer LG. Physical map of 1p36, placement of breakpoints in monosomy 1p36, and clinical characterization of the syndrome. Am J Hum Genet. 2003b; 72:1200–1212. [PubMed: 12687501]

Jiang H, Sha SH, Schacht J. Rac/Rho pathway regulates actin depolymerization induced by aminoglycoside antibiotics. J Neurosci Res. 2006; 83:1544–1551. [PubMed: 16521128]

Kent WJ. BLAT--the BLAST-like alignment tool. Genome Res. 2002; 12:656–664. [PubMed: 11932250]

Klaassen S, Probst S, Oechslin E, Gerull B, Krings G, Schuler P, Greutmann M, Hurlimann D, Yegitbasi M, Pons L, Gramlich M, Drenckhahn JD, Heuser A, Berger F, Jenni R, Thierfelder L. Mutations in sarcomere protein genes in left ventricular noncompaction. Circulation. 2008; 117:2893–2901. [PubMed: 18506004]

Lee JA, Carvalho CM, Lupski JR. A DNA replication mechanism for generating nonrecurrent rearrangements associated with genomic disorders. Cell. 2007; 131:1235–1247. [PubMed: 18160035]

Luedde M, Ehlermann P, Weichenhan D, Will R, Zeller R, Rupp S, Muller A, Steen H, Ivandic BT, Ulmer HE, Kern M, Katus HA, Frey N. Severe familial left ventricular non-compaction cardiomyopathy due to a novel troponin T (TNNT2) mutation. Cardiovasc Res. 2010

Markham, NR.; Zuker, M. UNAFold: software for nucleic acid folding and hybriziation. In: Keith, JM., editor. Bioinformatics, Volume II Structure, Functions and Applications. Totowa, N.J: Humana Press; 2008. p. 1-31.

Ming JE, Geiger E, James AC, Ciprero KL, Nimmakayalu M, Zhang Y, Huang A, Vaddi M, Rappaport E, Zackai EH, Shaikh TH. Rapid detection of submicroscopic chromosomal rearrangements in children with multiple congenital anomalies using high density oligonucleotide arrays. Hum Mutat. 2006; 27:467–473. [PubMed: 16619270]

Page SL, Shaffer LG. Nonhomologous Robertsonian translocations form predominantly during female meiosis. Nat Genet. 1997; 15:231–232. [PubMed: 9054929]

Popoff MR, Geny B. Multifaceted role of Rho, Rac, Cdc42 and Ras in intercellular junctions, lessons from toxins. Biochim Biophys Acta. 2009; 1788:797–812. [PubMed: 19366594]

Raghavan SC, Lieber MR. DNA structures at chromosomal translocation sites. Bioessays. 2006; 28:480–494. [PubMed: 16615081]

Redon R, Rio M, Gregory SG, Cooper RA, Fiegler H, Sanlaville D, Banerjee R, Scott C, Carr P, Langford C, Cormier-Daire V, Munnich A, Carter NP, Colleaux L. Tiling path resolution mapping of constitutional 1p36 deletions by array-CGH: contiguous gene deletion or “deletion with positional effect” syndrome? J Med Genet. 2005; 42:166–171. [PubMed: 15689456]

Rice P, Longden I, Bleasby A. EMBOSS: the European Molecular Biology Open Software Suite. Trends Genet. 2000; 16:276–277. [PubMed: 10827456]

Shaffer LG, McCaskill C, Han JY, Choo KH, Cutillo DM, Donnenfeld AE, Weiss L, Van Dyke DL. Molecular characterization of de novo secondary trisomy 13. Am J Hum Genet. 1994; 55:968–974. [PubMed: 7977360]

Thienpont B, Mertens L, Buyse G, Vermeesch JR, Devriendt K. Left-ventricular non-compaction in a patient with monosomy 1p36. Eur J Med Genet. 2007; 50:233–236. [PubMed: 17337261]

Wu SC, Solaro RJ. Protein kinase C zeta. A novel regulator of both phosphorylation and de-phosphorylation of cardiac sarcomeric proteins. J Biol Chem. 2007; 282:30691–30698. [PubMed: 17724026]

Zine A, Aubert A, Qiu J, Therianos S, Guillemot F, Kageyama R, de Ribaupierre F. Hes1 and Hes5 activities are required for the normal development of the hair cells in the mammalian inner ear. J Neurosci. 2001; 21:4712–4720. [PubMed: 11425898]

Figure 1.
Photograph of affected siblings. Patient 1 (upper right) is 4 years 7 months of age. Patient 2 (lower left) is 18 months of age. Midfacial hypoplasia, characteristic eyebrows, and upslanted palpebral fissues are notable.

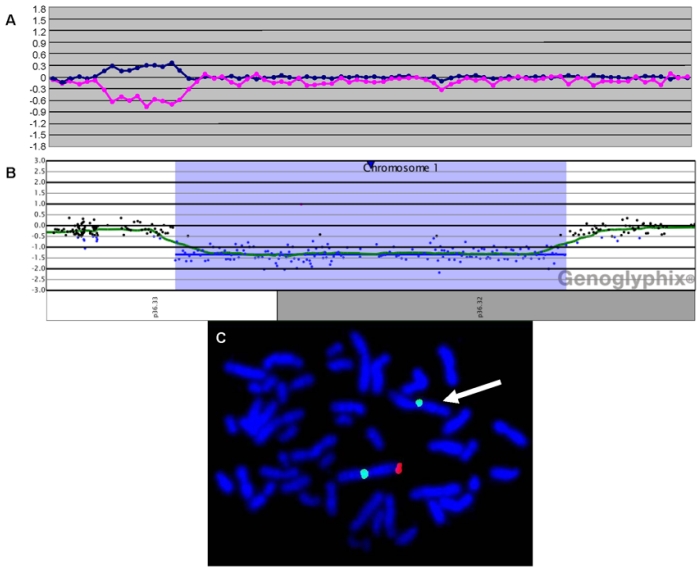

Figure 2.

Microarray and FISH analysis of interstitial deletions of 1p36.33p36.32. **(A)** BAC microarray plot for Patient 2 showing a single-copy loss of 11 BAC clones at 1p36.33p36.32, spanning ~1.4 Mb. Clones are arranged with the most distal p-arm clones on the left and the most distal q-arm clones on the right. The blue line is a plot of the array CGH data from the first microarray experiment (reference Cy5/patient Cy3). The pink line is a plot of the array CGH data from the second microarray experiment in which the dyes have been reversed (patient Cy5/reference Cy3). **(B)** Oligonucleotide microarray plot for Patient 2 showing a single-copy loss of 169 oligonucleotide probes at 1p36.33p36.32, approximately 1.51 Mb in size (chr1:1,906,449–3,419,622, hg18 coordinates). Oligonucleotide probes are ordered on the x axis according to physical mapping positions, with the most distal 1p36.33 probes to the left and the most proximal 1p36.32 probes to the right. (**C)** FISH in Patient 2 showing a deletion at 1p36.3. BAC clone RP11-740P5 from the deleted region is labeled in red, and the chromosome 1 centromere probe is labeled in green as a control. The presence of one red hybridization signal indicates deletion on one chromosome 1 homologue.

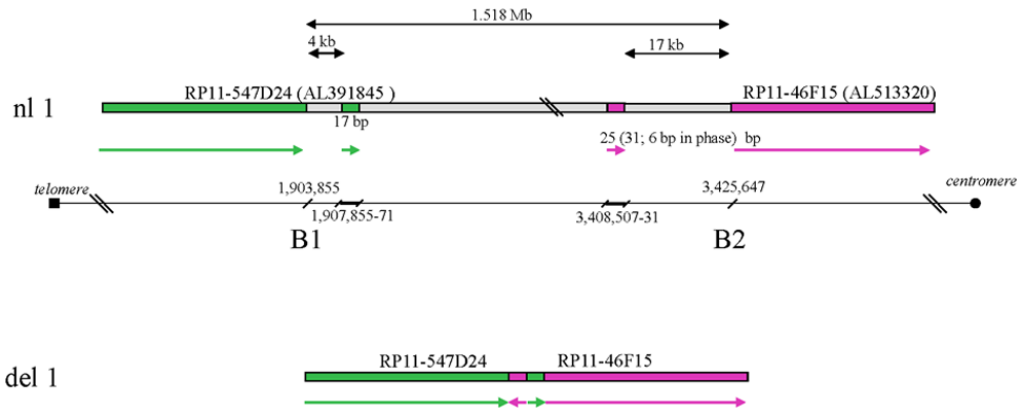

Figure 3.

Complex rearrangement found at the breakpoints in Patient 1 and Patient 2. Black horizontal line symbolizes chromosome 1p36 in the orientation from telomere (left) to the centromere (right). Localization of the breakpoints is indicated by DNA sequence positions in accordance with Mar. 2006 (hg18) assembly (UCSC). Nl 1 corresponds to normal chromosome 1, del 1 to chromosome 1 with the interstitial deletion. B1 indicates the distal breakpoint in the sequence (distal retained sequence is filled in green), while B2, the proximal breakpoint (proximal retained sequence is filled in magenta). Sequence fragments filled in grey indicate deleted sequence in del1. Two short sequence insertions (25 and 17 bp sequence fragments, respectively) were identified at the breakpoint junction. Both insertions originate from the 1p36 region localized between B1 and B2 as indicated at the figure. The 25 bp sequence fragment localized ~17 kb from the proximal breakpoint is in inverted orientation with respect to its progenitor, while the 17 bp inserted fragment derived from the more distal 1p36 region is in direct orientation with respect to its progenitor.

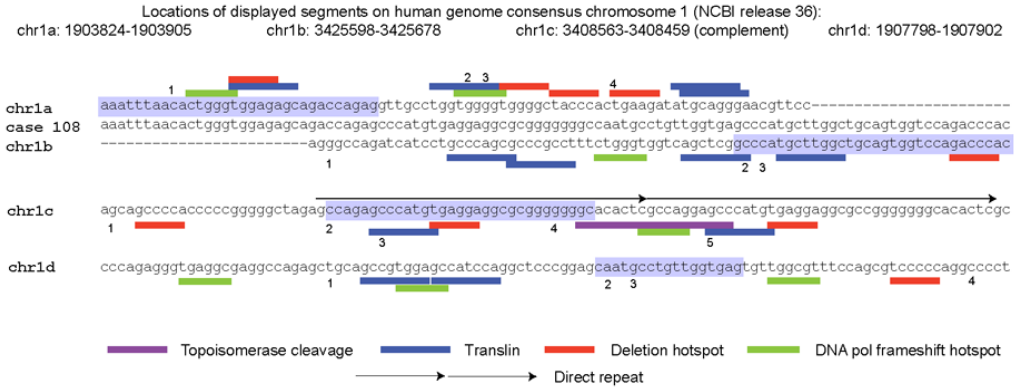

Figure 4.

Sequence analysis of the deletion breakpoints. The case is uncolored, while the 4 portions involved in the rearrangement (shown in blue) of normal chromosome 1 are colored where they align to the case sequence. Motifs are indicated by colored bars adjacent to the alignments: eukaryotic topoisomerase cleavage site consensus (magenta), translin (TSN) target motifs (blue), DNA polymerase frameshift hotspots (green), and deletion hotspot consensus (red). Paired arrows under a sequence indicate direct repeats (arrows in same direction). Numbers adjacent to the normal chromosome sequences indicate significant potential DNA structural features.

Table I

Primers used to sequence genes in the LVNC critical region. All designed at intron-exon junctions to amplify genomic DNA; small exons with small intervening introns were combined. Average amplicon lengths were 450 bp). All sequencing was done with both forward and reverse primers.

HES5	Exon 16
Exons 1 and 2	FOR 5’ CAC AAA GCC TTG CCA GAA GA 3’
FOR 5’ GCC AAT TCA CAG GCA ATT TA 3’	REV 5’ GCT CTT TAG GAA CCT GTG CT 3’
REV 5’ TAG TCC TGG TGC AGG CTC TT 3’	Exons 17 and 18
Exon 3	FOR 5’ TCA CAG CAA GGA GGC TTT 3’
FOR 5’ GAA GCA CAG CAA AGG TGA GC 3’	REV 5’ CAA TCA GGA GGA CAG ACA 3’
REV 5’ GCC CTG ATT GTC CTA AAA CG 3’	Exon 19
PANK4	FOR 5’ TGC TGT CCA CAC AAA CTA CCA 3’
Exon 1	REV 5’ ATG AAC GTC TCC CAG GAC AA 3’
FOR 5’ TCA GTC CAG ATG TTC TGT GC 3’	**SKI**
REV 5’ CGA TGT GGC CGA AGA CAT AA 3’	(Exon 1 was divided into 3 overlapping amplicons based on its size)
Exons 2 and 3	Exon 1A
FOR 5’ GCT GAG GAG GAG CAG AAT TT 3’	FOR 5’ ACG CAG GGC AAC AAA CAG 3’
REV 5’ CCC TTA ATC AAG CAC GTC AT 3’	REV 5’ TTG GCG CTC TCC TTC TTG TA 3’
Exon 4	Exon 1B
FOR 5’ ATC TCA AGG GCG AGA AAG GA 3’	FOR 5’ CAG AAG ACG CTG GAG CAG TT 3’
REV 5’ CAG CGA GGG CTT AAC AAA CT 3’	REV 5’ AGG ATG CCC ATG ACT TTG AG 3’
Exon 5	Exon 1C
FOR 5’ AAG GTA AGA CCC GGC TTC AT 3’	FOR 5’ TGC CGC AGA TTC TCA ACT C 3’
REV 5’ CCA CCC AGC CAG GAT AGA A 3’	REV 5’ TTC GGA GAC CAG AGC CTG TA 3’
Exons 6 and 7	Exon 2
FOR 5’ AGC AAC CCA GAG CTT CTA TC 3’	FOR 5’ TGA CTT GTC CCT CAG CAC AG 3’
REV 5’ CAC GGT GCC ACA AAA TGT AG 3’	REV 5’ CAC TCA CCT GTC TCG GAT GA 3’
Exons 8 and 9	Exon 3
FOR 5’ CTA CAT TTT GG GCA CCG TG 3’	FOR 5’ GGG ACA TGA AGT GGC TTG TT 3’
REV 5’ AAA GCA AGC CAC AGT GTC CT 3’	REV 5’ TTC TGC TTG CTG GGT CTC TT 3’
Exon 10	Exon 4

FOR 5’ CAA ACC AGG GGG TAA GTC AA 3’	FOR 5’ AGA GAC CCA GCA AGC AGA AA 3’
REV 5’ CAG ATC AAG GGG TTT CTG GA 3’	REV 5’ GCA CAG AAA GCG ACT CAC AC 3’
Exons 11 and 12	Exon 5
FOR 5’ TCA GCC TTT CCT GTT CCA GT 3’	FOR 5’ CCA TGT TTC GCA GGT TCC TC 3’
REV 5’ AAC ACA GCT CCT CAG CAG AT 3’	REV 3’ ACA CTG AGG GGC TCA CCA TA 3’
Exon 13	Exon 6
FOR 5’ CTG AGT CTT CGA TCC TGA 3’	FOR 5’ CCA GGG CAC ATT GTC AGA TA 3’
REV 5’ TGC GGC ACC CAT GCT TAA 3’	REV 5’ TCC TCC ACC TCG TAG GAC AC 3’
Exons 14 and 15	Exon 7
FOR 5’ AGT GAT TTG GGG TCT TCA CG 3’	FOR 5’ TCT CGT GAG CCT GTG TCC TA 3’
REV 5’ TCT TCT GGC AAG GCT TTG TG 3’	REV 5’ AAT GTT CCA GCA AGC AGA GG 3’

Table II

Genes within the deleted region.

Gene Name	OMIM number	Description	Function	Human mutations
KIAA1751		Hypothetical protein LOC85452	Unknown	NR
GABRD	137163	Gamma-aminobutyric acid receptor, delta	Inhibitory neurotransmitter (GABA) receptor	Generalized epilepsy with febrile seizures plus, juvenile myoclonic epilepsy, and idiopathic generalized epilepsy [Dibbens et al., 2004]
PRKCZ	176982	Protein kinase C, zeta form	Kinase with roles in brain, heart, immune function, and glucose transport; Wnt pathway	NR
C1orf86		Chromosome 1 open reading frame 86	Unknown	NR
LOC100128003		Hypothetical protein LOC100128003	Unknown	NR
SKI	164780	V-Ski avian sarcoma viral oncogene homolog	Proto-oncogene promoting cell growth in many tissues; TGF-β and BMP pathways	NR
MORN1		MORN repeat containing 1	Unknown	NR
LOC100129534		Small nuclear ribonucleoprotein polypeptide N pseudogene	Pseudogene	NR
RER1		Retention in endoplasmic reticulum 1 homolog (S. cerevisiae)	Transmembrane golgi protein involved in the retention of endoplasmic reticulum membrane proteins; facilitates gamma-secretase complex assembly	NR
PEX10	602859	Peroxisome biogenesis factor 10	Ubiquitination of peroxisome import receptor	Zellweger spectrum disorders (AR)
PLCH2	612836	Phospholipase C, eta-2	PIP2 hydrolysis, sensitive to Ca2+ concentration; neuronal	NR
PANK4	606162	Pantothenate kinase 4	Regulation of CoA biosynthesis, mainly in muscle	NR
HES5	607348	Hairy/enhancer of split, Drosophila, homolog of, 5	Transcriptional repressor in the NOTCH pathway; expressed in developing brain, heart, and ear	NR
LOC115110		Hypothetical protein LOC115110	Non-coding RNA	NR
TNFRSF14	602746	Tumor necrosis factor receptor superfamily, member 14	Regulation of T-cell responses, activation of NF-kappa-B	NR
C1orf93		Chromosome 1 open reading frame 93	Unknown	NR
MMEL1		Membrane metallo-endopeptidase-like 1	Secreted (soluble and membrane-bound versions) peptidase with strongest testes expression	NR
ACTRT2	608535	Actin-related protein T2	Cytoskeletal organization	NR
FLJ42875		Hypothetical LOC440556	Non-coding RNA	NR
PRDM16	605557	PR domain-containing protein 16	Transcriptional regulation; TGF-β and BMP pathways; stimulates brown adipogenesis; role in palate and craniofacial development	NR
ARHGEF16		Rho guanine exchange factor (GEF) 16	Role in rho GTPase-mediated signalling	NR

Gene Name	OMIM number	Description	Function	Human mutations
MEGF6	604266	Multiple epidermal growth factor-like domains 6	Secreted; exact function unknown	NR

NR = None reported; AR = autosomal recessive